

GraphMoco: a Graph Momentum Contrast Model that Using Multimodal Structure Information for Large-scale Binary Function Representation Learning

Sun RuiJin^a, Guo ShiZe^c, Guo Xi^b, Pan ZhiSong^a

^a*Army Engineering University of PLA*

^b*University Of Science & Technology Beijing*

^c*National Computer Network and Information Security Management Center*

Abstract

The ability to compute similarity scores of binary code at the function level is essential for cyber security. A single binary file can contain tens of thousands of functions. A deployable learning framework for cybersecurity applications needs to work not only accurately but also efficiently with large amounts of data. Traditional methods suffer from two drawbacks. First, it is very difficult to annotate different pairs of functions with accurate labels. These supervised learning methods can easily be overtrained with inaccurate labels. The second is that they either use the pre-trained encoder or use the fine-grained graph comparison. However, these methods have shortcomings in terms of time or memory consumption. We focus on large-scale Binary Code Similarity Detection (BCSD) and to mitigate the traditional problems, we propose GraphMoco: a graph momentum contrast model that uses multimodal structure information for large-scale binary function representation learning. We take an unsupervised learning approach and make full use of the structural information in the binary code. It does not require manually labelled similar or dissimilar information. Our models perform efficiently on large amounts of training data. Our experimental results show that our method outperforms the state-of-the-art in terms of accuracy.

*Fully documented templates are available in the elsarticle package on CTAN.

Keywords: Binary code similarity detection, Contrastive Learning,
Embedding, Cyberspace security
2010 MSC: 00-01, 99-00

1. Introduction

Given a set of function pairs, binary code similarity detection (BCSD) focuses on whether we can determine that these function pairs are semantically consistent. Binary files are often compiled from high-level languages. Files with the same semantic meaning are often literally very different. BCSD has important applications in many areas of cybersecurity. If the library files you use are vulnerable, BCSD will help you find them. If patches have been applied, BCSD can provide a reference to where the patches are. When analysing malicious code, BCSD can help you to tag malicious code with family information.

With the development of deep neural networks, more and more people are using deep neural networks in this area. In particular, the development of graph neural networks and natural language processing has helped BCSD a lot. Both academia and industry are heavily involved in this area of research. But there are still many gaps in the existing research.

First, most of the articles adapt supervised learning models [24] [21] [16][36] [36], and they all suffer from the difficulty of labelling. When we are given a set of binary functions, we need to label them before training. To label the distance between different functions, some distance functions are used, such as edit distance[28], cosine similarity [21]. As it is often difficult to obtain binary source code, marking binary files often requires trained professionals and takes a lot of time. People label the distance between the two similar functions as $\{1\}$ and the distance between two different functions as $\{-1\}$ or $\{0\}$. But the mutual information between any pair of functions cannot be -1 or 0 . For example, we might mark *writefile()* and *appendfile()* as $\{0\}$ because they are not the same function. But in fact these two functions are very similar, the ground truth should be a score between 0 and 1. It is difficult for us to find a reasonable

number to label each of the different function pairs. If we use $\{0\}$ to label them, it can lead to overtraining, which causes slow convergence as mentioned in [27].

Second, with large amounts of data a practical system must be able to work not only accurately but also efficiently. To improve accuracy, people resort to complex models. However, these models have excessive computational and memory requirements, which affects their generality. This is because a single binary file can contain tens of thousands of functions [20]. The size of the functions also varies greatly, a single binary function may contain hundreds of nodes and thousands of instructions. When faced with large amounts of data, existing models work accurately but not efficiently. Take the existing state-of-the-art (SOTA) model GMN and Order Matters [38] for example, GMN [18] makes similarity judgments about function pairs on a fine-grained comparison, which requires a large amount of computation. When computing the similarity score between a new graph and all graphs, the GMN must share all information about the new graph with all graphs in the database. For large amounts of data, this algorithm is time consuming. Yu et al. [38] uses the BERT-base model to encode the node-level embeddings, and then sums these embeddings for the function graph. With thousands of nodes of a single binary, the memory consumption is too high. The consumption of these models is proportional to the number of nodes or instructions of the function. They are too computationally and memory intensive despite their high accuracy. We need a model that can be applied efficiently.

We look for solutions that are not only accurate but also efficient. Inspired by recent advances in the fields of graph neural networks [23], contrastive learning [10] and NLP, by taking full advantage of the structural features of the different layers, we propose GraphMoco: a graph momentum contrast model that uses multimodal structural information for large-scale binary function representation learning. In our model, we encode code at the token levels, block levels and graph levels respectively. We then fine-tune the encoder with contrastive learning modules. We have also extensively tested the model, and the experimental results show that our algorithm can significantly improve the accuracy while

effectively reducing the amount of computation and memory consumption. We conclude that GraphMoco can efficiently generate high-quality binary embeddings, and we hope that GraphMoco will be helpful for various downstream binary analysis and graph embedding tasks.

In summary, the contributions we have made are as follows:

- 1, At the token level, we propose an innovative cross-platform representation model `asm2vecPlus`. It consists of an instruction normalization procedure and an instruction embedding learning network. The model could learn the instruction embeddings, which contain rich semantic information, and reduce out-of-vocabulary (OOV) problems by taking advantage of the structural features.
- 2, At the block-level, a multimodal CNN encoding scheme `StrandCNN` is used to produce the embeddings. CNN are used to capture the strand of binary and a variety of mechanisms are used to optimise the model by taking full advantage of the structural features of the binary. The embedding is then sent to the high order graph encoder.
- 3, We have developed a graph momentum learning model to optimise the encoder. It is a siamese network with a embedding queue. We design a preshuffle mechanism to solve the information leakage problem.
- 4, By building a large and consistent queue, we can train the model by using less memory and contrasting loss functions in large batches. The model can also be applied to other areas of graph contrastive learning.
- 5, We have tested our model on several datasets. Our model outperform the SOTA models on several metrics.
- 6, To facilitate further research, we have made our code publicly available at <https://github.com/iamawhalez/GraphMoco>.

2. Background and Related Work

The definition of BCSD and related work is briefly presented in this section.

2.1. Definition of BCSD

Most software is not built from scratch. There are a lot of clones in the underlying assembly code since different source codes are frequently reused throughout the development of the program. The following is a definition of Binary Code Similarity Detection (BCSD). Without having access to source code or compilation information, if we are given two pieces of binary code, we may determine whether the two pieces of code are the similar. The similarity is referred to as semantic consistency. It means that although the characters in the two pieces of code may be different, their semantics are the same. Even if two functions are compiled with the different optimisations and come from the different architectures, they will behave identically when given the same input. BCSD methods can generally be divided into two types. One is based on features and the other is based on embeddings. We will describe these two methods in detail.

2.2. BCSD Based on Features

Traditional BCSD methods rely heavily on some specific features or structures. The earliest binary file similarity comparison tool is named EXEDIFF [2], released in 1999, and is used to determine the patch information of different versions of executable files. They mainly use the structure information of disassembled code. String-based detection methods are the most basic ones [3] [4]. They use the string or string edit distance to find duplicates. *n-grams* is another commonly used feature [13], they are the contents of a sliding window of size N in bytes. DiscovRe[9] defines some features that are less affected by different architectures and extracts statistical features to represent each basic block.

2.3. BCSD Based on Embeddings

Embedding is the transformation of discrete variables into a high-dimensional continuous space. In embedding-based solutions, functions are compared not by the character of the functions, but by the learned embedding of the functions.

They first transform the binary functions into multi-dimensional vector representations (embeddings). They then compare the two vectors using simple geometric operations[21]. Functions with similar semantics have embeddings close to each other in the high-dimensional space.

There are 3 ways of learning the instruction-level embedding. First type is SAFE[21], SAFE ignores the internal structure of the assembly code. In their dictionaries, instructions with the same operand and different opcodes are encoded into unrelated integer. In SAFE, dictionaries can be oversized by up to 100,000. New instructions are considered to be out-of-vocabulary, but in fact they are just combinations of different operands and operations. Second is [17], which treats the instructions as sentences and use the BERT[6] to learn the embedding. This model suffers from excessive memory consumption. The third model is Asm2vec, which makes better use of the internal structure of the instructions. Asm2Vec [8] learns the embedding of operands and operation symbols separately and then concat them together. But Asm2vec model can only handle code for x86 architectures.

With the development of Graph Neural Networks, more and more articles use GNN to obtain the embeddings of functions. In the graph-based embedding model, the embeddings of the nodes are obtained first. Statistical features are a common way of encoding at block level, Xu et al. [36] uses 8 statistical features. [20] uses the frequency of two hundred assembly instructions. The existing model uses statistical features to avoid the problem of high memory requirements. However, these simple models may lead to a lack of accuracy. Having obtained the node-level embedding, the PDG or CFG information can be used to obtain the embedding of the entire function. A Program Dependency Graph (PDG) is a graphical representation of the data and control dependencies within a procedure [19]. It was used in program slicing at first [37]. More people use CFG(Control Flow Graph), such as [26] and [25]. They may transform the binary code into CFGs, and use a graph analysis algorithm to find the similarity. GMN [18] computes a similarity score between them by jointly reasoning on the pair through a new cross-graph attention-based matching mechanism. For large

samples, GMN requires a comparison of each function pair at the node level. Existing models are inadequate in terms of accuracy or time complexity.

If we compare assembly code instructions to words and functions to sentences, then the BCSD problem can be solved by using NLP techniques. With the success of pure attention networks in the NLP domain such as Transformer [32] and BERT [7], more and more models are adopting Transformer-like structures in BCSD. These articles [16] [17] [24][38][1] all adopt the structure based on the pure attention pre-training model and achieve a very excellent effect. Yu et al. [38] uses a method based on BERT. In particular, they use BERT to pre-train the binary code at the one-token level and one-block levels. Then they use convolutional neural networks (CNN) on adjacency matrices to extract the order information. PalmTree [17] utilizes three pre-training tasks to capture various characteristics of assembly language and generate general-purpose instruction embeddings by performing self-supervised training on large-scale unlabelled binary corpora. TREX [24] develops a novel neural architecture, a hierarchical transformer, which can learn execution semantics from micro-traces during the pre-training phase.

3. Problem Definition and Solution Overview

3.1. The Basic Definition

In order to describe our problem clearly, we have started with a brief description of the symbols defined. Throughout this paper, we will use the following mathematical notation.

x		one binary function to be classified
X		the binary function dataset
\vec{f}_b		embedding vector of block-level
\vec{f}_g		embedding vector of graph-level
d		is the distance function of two embeddings

When we are given two binary functions x_1, x_2 , if x_1, x_2 are compiled from the same source code. We say that they are similar. We aim to design a DNNs

based encoder f . when we put x_1, x_2 into the same encoder f , two embeddings $f(\vec{x}_1), f(\vec{x}_2)$ are produced. If x_1, x_2 are similar, we want the distance of two embeddings $f(\vec{x}_1), f(\vec{x}_2)$ within a certain threshold $d(f(\vec{x}_1), f(\vec{x}_2)) < threshold$. If x_1, x_2 are not similar, opposite is true $d(f(\vec{x}_1), f(\vec{x}_2)) > threshold$. d is a distance function.

3.2. General Framework

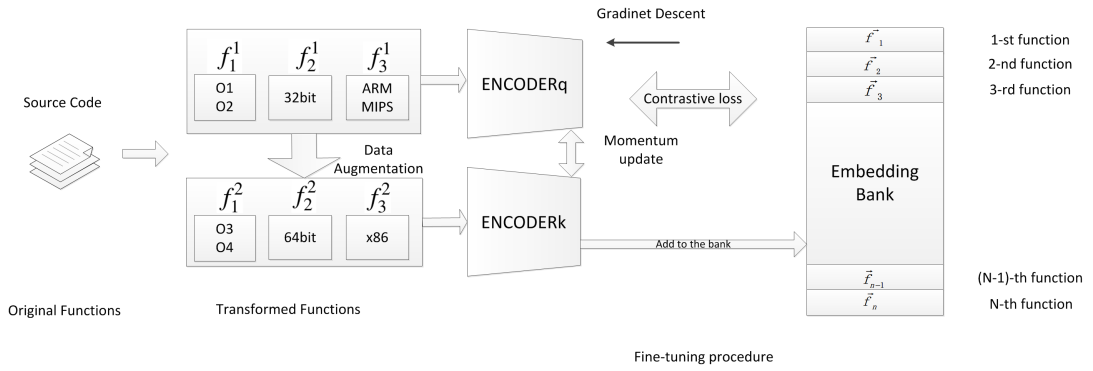


Figure 1: The framework of the proposed unsupervised learning method GraphMoco. It consists of a data augmentation part, a siamese network encoder and an embedding queue. The input function pairs are projected into a low-dimensional normalized embedding with the DNN based encoders. The query encoder (encoderq) is updated by back-propagation and the key encoder(encoderk) is updated by momentum.

In this section, we present GraphMoco: a Graph Momentum Contrast model that uses multimodel structure information for large-scale binary function representation learning, and discuss the technical approach behind it. We start by describing the general algorithm, and then briefly introduce the main parts of the model. Our model is a siamese graph embedding network with an embedding queue as shown in Figure 1.

The GraphMoco model consists of the following parts.

- First, a data set X and the sample augmentation module $Trans(\cdot)$.
- Second, a representation learning model at the instruction level, namely Asm2VecPlus. It can learn the representation of operands and operators.

$f_i(\cdot)$.

- Third, $f_b(\cdot)$ is a block-level representation learning model, we call it Strand-CNN. It can learn the representation of each block of binary CFG.
- Fourth, a GNN encoder. At the graph level, our use of higher order graph neural networks[23] $f_g(\cdot)$ allows us to exploit the structural information of graph neural networks while exploiting the statistical information of graphs.
- Finally, the contrastive learning module, which consists of a distance function $d(\cdot)$, a loss function $\ell(\cdot)$ and an embedding queue *queue*.

Because we're using the contrastive learning model, we don't need dissimilar pairs to train the model. Given a function x_i in the original dataset X , the augmented data could be produced by passing the original x_i to the data augmentation module $Trans(\cdot)$. We could get two augmented binary functions, x_i^1 and x_i^2 . The CFG of x_i^1 and x_i^2 are then produced. Each graph can be divided into blocks, and each block can be divided into instructions. For each instruction ι_i , the embedding $\vec{\iota}_i$ are learned by Asm2VecPlus. For each block, we use the instruction embedding $\vec{\iota}_i$ and the StandCNN model to learn the block-level embedding \vec{b}_i , and finally we get the graph-level embedding $f(\vec{x}_i)$ by the GNN model.

There are two encoders in GraphMoco. they are the *query* encoder and the *key* encoder. When an example x is sampled, the augmented function-pair x_i^1 and x_i^2 are produced. They are sent to two encoders separately. The query encoder $f(\vec{\cdot})_q$ is used to generate the query embeddings $f(\vec{x}_i^1)_q$. The key encoder $f(\vec{\cdot})_k$ are used to produce the key embeddings $f(\vec{x}_i^2)_k$. The key embeddings are added to the embedding queue. We treat each function instance as a separate class of its own and train a classifier to discriminate between individual instance classes. The encoded query embedding $f(\vec{x}_i^1)_q$ should be similar to its matching key embedding $f(\vec{x}_i^2)_k$ and dissimilar to others in the key embeddings queue. The query encoder is updated by gradient and the key encoder is updated by a

momentum update, as explained in Section 4.

We then use the contrastive learning module to optimize the encoder.

4. Details of the Model

If we disassemble the function into CFG, we can consider the basic blocks as sentences and the instructions of the blocks as words. NLP and GNN techniques can be applied to BCSD. Asm2vecPlus is used to learn the embedding of instructions and StrandCNN is used to learn the embedding of blocks. We use GNN to learn the embedding of functions. Finally, GraphMoco are used to optimise the encoder.

4.1. Data Augmentation Strategies

The role of the data augmentation module in contrastive learning is very critical. In the realm of binary code, each assembly has a specific meaning. Given a binary function code, we could produce different binaries with the same semantics. These binaries may be suitable for different architectures or obfuscated or compiled with different optimizations. We explore different data augmentation strategies, including different architecture, different optimization and different bitness.

In general, we randomly select the CPU platform on which the code will run. There are two main parameters, the architectures of the CPU and the width of the CPU. The architectures we support include x86-32, x86-64, arm-32, arm-64, mips-32 and mips-64. Our model includes common mainstream CPU types. The assembly codes produced by different compilation options for the same function written in the same high-level language are also very different. Given a specific function, we will compile these functions with different compilers *i.e.* ,*clang*, *gcc* and with different optimization options, *i.e.* ,*O0*, *O1*, *O2* and *O3*.

4.2. Embedding learning

GraphMoco first extracts binary functions into the form of an Attributed Control Flow Graph (ACFG). In an ACFG, each vertex is a basic block labeled with a set of instructions. Each basic block has only one entry and one exit. We use GNN to learn the embedding of functions. The overall process of the encoder is shown in Figure 2.

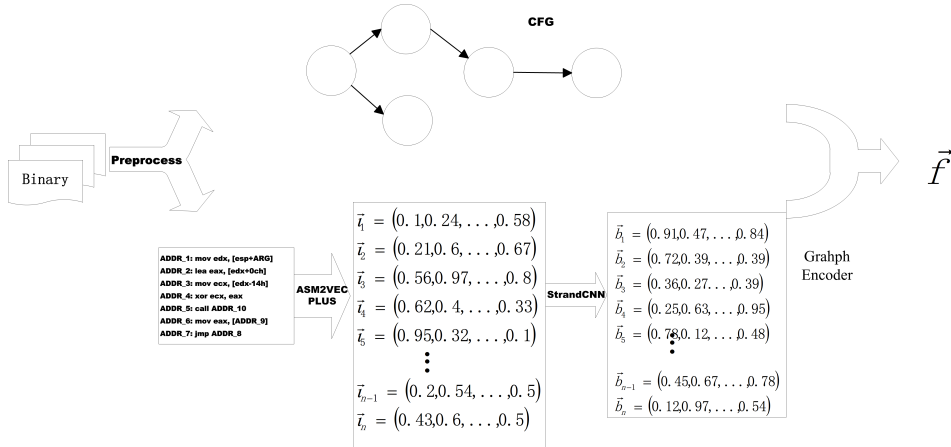


Figure 2: The figure shows the general steps for the complete encoder. Binaries are preprocessed into ACFG. The embedding of each block are learned by the block-level encoder. Then the block-level embedding and the CFG feature are used by the graph encoder to produce the function embedding.

4.2.1. Asm2vecPlus: Instruction Representation Learning Module

The first step of our solution is to associate an embedding vector with each instruction. Many people adopt [33][24][38] the the state-of-the-art pre-trained language model-BERT. However, the memory consumption of the BERT-based model is huge and it can not take full advantage of the latent lexical semantic structure of the assembly instruction. Assembly instruction has a fixed structure. For each instruction, there is generally an operation symbol and a number of operands. The number of operands varies from 0 to more than 10. Asm2vecPlus is based on the Asm2vec [8] architecture which is an extension of

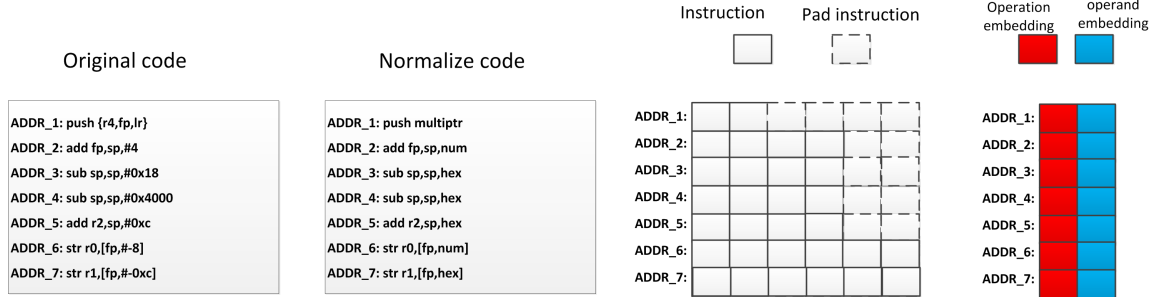


Figure 3: The diagram shows the steps for the model Asm2vecPlus model to generate the embedding for each instruction. The original codes are normalized and padded to the fixed length. Then the operations and the oprands are projected into embeddings seperately. We add the oprands embeddings together and concat with the embedding of the operation.

the original word2vec[22] model. We extended the Asm2vec model to accommodate multiple CPU architectures. The overall flow of the model is shown in the Figure 3.

Asm2vecPlus maps each repository instruction to a vector $\vec{l}_i \in \mathbb{R}^{2d}$. First, instructions must be normalize to mitigate the OOV problem.

- (1) To prevent the vocabulary list from becoming too large, we replace string, numbers, etc. in the assembly instruction with the special symbol **IMM**.
- (2) We replace the function address within the scope of the function as **ouraddress**, and function address outside the scope of the function as **inaddress**.
- (3) We replace the curly brackets and all the register within the brackets with symbol **Register**. We found that an ARM multi-register transfer instruction can process any subset of the 16 visible registers with a single instruction. This normalization greatly reduces the length of the instructions.
- (4) For ease of use, all the assembly instructions are padded to a fixed length. After the normalization, the dictionary of the code could be learned. For each instruction, the embedding that we will learn is $\vec{l}_i \in \mathbb{R}^{2d}$. Each instruction contains a list of operands $\vec{operand}_i^k \in \mathbb{R}^d$ and one operation $\vec{operation}_i \in \mathbb{R}^d$. Operands and operations are treated separately. We map each *operation* into a numeric vector $\vec{operation}_i \in \mathbb{R}^d$. If there are n oprands in the i -th instruction, we

could map each $operand_i^k$, $k \in n$ into a numeric vector $\vec{operand}_i^k \in \mathbb{R}^d$. All the $\vec{operand}_i^k$ are summed as the embeddings of operands, $\vec{operand}_i = \sum_{k=0}^n \vec{operand}_i^k$ and concatenated with the operation embedding $\vec{operation}_i$.

After the concatenation, the embedding of i -th instruction is denoted as $\vec{t}_i = \vec{operation}_i \parallel \sum_{k=0}^n \vec{operand}_i^k$.

4.2.2. Block Representation Learning Module

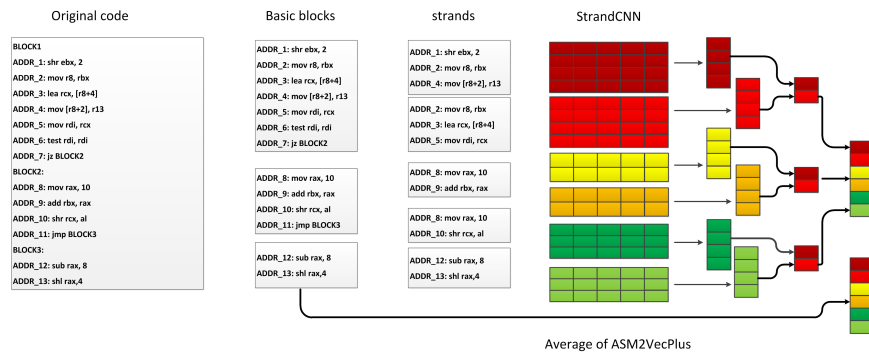


Figure 4: Illustration of the steps for the StrandCNN model. It is a slight modification of TEXTCNN. The model consists of two parts. In the first part, strand embeddings are learned by convolutions of different sizes. In the second part, the average instruction embedding is used to represent the general information of the block. Finally, two embeddings are concatenated together.

Having obtained the embedding representation of each instruction, we use this as the basis for obtaining block-level embeddings. As shown in figure 4, the model architecture is a slight variant of the TEXTCNN[15], we name it StrandCNN. A basic block is a sequence of codes with only one entry point and only one exit[27]. A strand is the set of instructions from a block that are required to compute the value of a particular variable [5][30]. [5] [30] decompose procedures into strands and use strands to establish similarity between procedures. Instructions in the same strand are often not far apart, and this is a local structural feature of the binary. We believe that convolution with a filter could learn the strands. Inspired by the [15][5][30], we use the convolutional neural network(CNN) to capture strands and build on the strands to learn block-level

embedding.

let $\vec{l}_i \in \mathbb{R}^{2d}$ be the i -th instruction of the block. A block of length n instructions is represented as $\vec{l}_1 \parallel \vec{l}_2 \parallel \vec{l}_3 \parallel \dots \parallel \vec{l}_n$. In general, let $\iota_{i:i+j}$ refer to the concatenation of instruction embeddings $\vec{l}_i \parallel \vec{l}_{i+1} \parallel \dots \parallel \vec{l}_{i+j}$. Most of the instructions in the same strand are not far apart from each other. As shown in Figure 4, the length of all the strands is less than 5. We use a convolution with a filter $w \in \mathbb{R}^{hd}$ to produce a new feature, where h is the size of the windows. We set the $h \leq 5$ in our article and the length is capable of learning most of the features. For example, a feature c_i is generated from a window of instructions $\iota_{i:i+h-1}$ by $c_i = \text{Activate}(W \cdot \iota_{i:i+h-1} + b)$.

Here $b \in \mathbb{R}^k$ is a bias term and $\text{Activate}()$ is an activation functions such as the hyperbolic tangent. This filter is applied to each possible instruction window in the block $\vec{l}_1 \parallel \vec{l}_2 \parallel \vec{l}_3 \parallel \dots \parallel \vec{l}_n$ to produce a feature map $\text{cmax}[i] = \max\{c_1, c_2, c_3, \dots, c_n\}$.

We then apply a max pooling operation on the feature map. The idea is to capture the most important strands. We have described the process by which one strand is extracted. The model uses multiple filters (with different window sizes) to obtain multiple strands. We concatenate all the strands feature together. At last, we average the instructions embedding of the block by Asm2VecPlus and concatenate it with strands feature as the final embedding of the block.

4.2.3. Function Representation Learning Module

Once the block-level representation have been learned, we use GNNs to get the function-level embeddings. Traditional GNNs cannot be more powerful than the 1-WL[35][23]. We turn to the k -dimensional GNNs (k -GNNs). k -GNNs is based on the k -dimensional WL algorithm, which can take into account higher-order graph structures.

The CFG of the assembly code has distinct structural features, as shown in the diagram, and both code segments are branches of the IF statement. In the CFG diagram, there is similarity in the relationships of the different nodes. We believe that similar code have similar subgraph structures.

4.3. Contrastive Learning Module

In this section, we describe in detail the contrastive learning module, which consists of a distance function, a loss function, a siamese encoder network and an embedding queue. The goal is training a representation encoder by matching an encoded query to a dictionary of encoded keys using a contrastive loss.

4.3.1. Siamese Network and the Embedding Queue

When one example x_i is sampled, then the augmented function-pair x_i^1 and x_i^2 is produced. The augmented functions are sent to the siamese network, they are the query encoder $f(\vec{\cdot})_q$ and the key encoder $f(\vec{\cdot})_k$. The key encoder is used to generate the key embedding, the key embedding will be added to the key embedding queue. The query encoder $f(\vec{\cdot})_q$ is used to generate the query embedding $f(\vec{x}_i)_q$. The query embedding $f(\vec{x}_i)_q$ should be similar to its matching key embedding $f(\vec{x}_i)_k$ and dissimilar to all the others in the key embedding queue. By maintaining the queue, the query embedding can be compared with more embedding keys, allowing for a larger batch to be trained with less memory. And it leads to better training results. The loss is calculated by InfoNCE [31]. The query encoder updates parameters by gradient descent and the key encoder will be updated by the momentum update mechanism as mentioned in Section 4.3.3.

4.3.2. Loss Function

We assume that all the samples are different, BSCD could be transformed into an instance discrimination problem [34]. All the key embedding in the queue is $\vec{k}_0, \vec{k}_1, \dots, \vec{k}_n$. If an query embedding $vecq$ is given, there is only one single key that matches $vecq$ (denoted as \vec{k}_q). we formulate the probability that any embedding \vec{k}_i belongs to the i -th function using the softmax-like criterion.

$$P(k_i | \mathbf{q}) = \frac{\exp(\mathbf{k}_i^T \mathbf{q})}{\sum_{j=1}^n \exp(\mathbf{k}_j^T \mathbf{q})} \quad (1)$$

where $P(k_i | \mathbf{q})$ means the probability that q belongs to class i . We also introduce a temperature parameter τ which controls the concentration level [11].

The probability $P(k_i | \mathbf{q})$ becomes:

$$P(k_i | \mathbf{q}) = \frac{\exp(\mathbf{k}_i^T \mathbf{q}) / \tau}{\sum_{j=1}^n \exp(\mathbf{k}_j^T \mathbf{q}) / \tau} \quad (2)$$

We aim to maximize probability $P(k_i | \mathbf{q})$. It equivalently minimizes the negative log-likelihood $-\log P(k_i | \mathbf{q})$. The loss function becomes the InfoNCE loss [31]. The goal of fine-tuning is to minimize it.

$$\ell_{oss} = -\log P(k_i | \mathbf{q}) = -\log \frac{\exp(\mathbf{k}_i^T \mathbf{q}) / \tau}{\sum_{j=1}^n \exp(\mathbf{k}_j^T \mathbf{q}) / \tau} \quad (3)$$

By minimizing the loss function ℓ , we can minimize the distance between the augmented function pair, and we can maximize the cosine distance between different functions. In this way, the goal of function classification can be achieved without labeling samples of different types.

4.3.3. Momentum Update

$$P(k_i | \mathbf{q}) = \frac{\exp(\mathbf{k}_i^T \mathbf{q})}{\sum_{j=1}^{all} \exp(\mathbf{k}_j^T \mathbf{q})} \quad (4)$$

Given the query function q , the perfect models could exactly distinguish the corresponding key embedding k_i from all the other embeddings in the queue. It is equivalent to replacing n in Equation 1 with the number of the dataset *all*, as shown in the Equation 4. We can see that good features can be learned by a large dictionary that covers all the negative samples. If it is not possible to cover all the examples, the more the negative samples are covered, the better result will be learned.

So the core of our approach is maintaining the key embeddings queue. Our solution is based on Moco which is introduced in [10]. Maintaining a embedding queue can learn good features with less memory consumption, but it also makes it intractable to update the key encoder by back-propagation. We use the momentum update mechanism.

$$\theta_k \leftarrow m * \theta_k + (1 - m) * \theta_q \quad (5)$$

θ_q are the parameters of the query encoder, θ_k are the parameters of the key encoder, the encoders are initialized with the same parameters. In each round of training, the loss is calculated by Equation 3. Only the parameters θ_q of the query encoder are updated by back-propagation. The parameters θ_k are updated by momentum as shown in Equation 5. Here $m \in [0, 1)$ is a momentum coefficient.

4.3.4. Preshuffle Mechanism

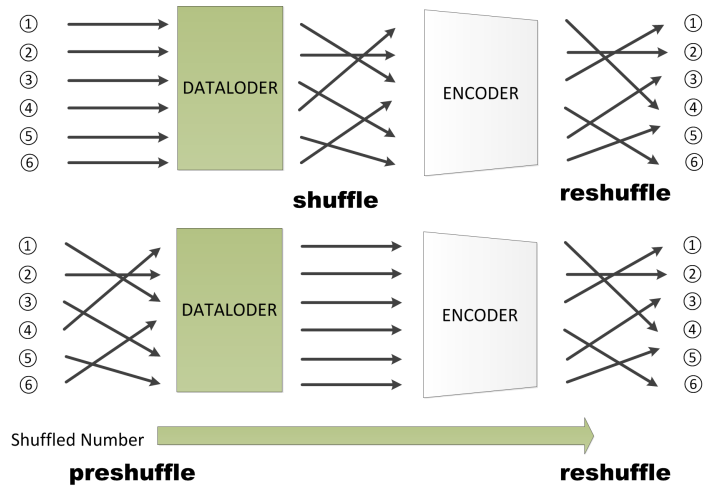


Figure 5: The illustration of the difference between the preshuffle mechanism and the shuffle BN mechanism proposed by [10]. Shuffle is used before the data is sent to the encoder. Preshuffle is used at the dataloader step and the shuffled index is sent as a parameter to the encoder.

Moco[10] found that Batch Normal mechanism[12] prevents the model from learning good representations, they shuffle the order of the batch to prevent Moco from learning the cheating low-loss solution. Our encoder doesn't contain a BN layer, but GraphMoco still learned the cheating solution when it is trained on one single GPU. As for GNN related encoders, all the graphs in one batch must be reconstructed into a new single graph and sent to the encoder, and the original shuffling mechanism doesn't work in GNN. We propose the preshuffle mechanism. The graphs of the batch are shuffled when we pack the dataset and

the shuffled the number considered as a new parameter. After the embedding are learned by the encoder, the batch are reshuffled.

4.3.5. Distance Function

We use the cosine distance function $sim()$ to judge the similarity of function pairs. Given a pair of functions x_1 and x_2 , $f(\vec{x}_1)$ and $f(\vec{x}_2)$ are the embedding vectors produced by the encoder. We could use the cosine similarity as the distance metric d . The cosine similarity formula is shown below:

$$d(x_1, x_2) = sim(x_1, x_2) = \frac{f(\vec{x}_1)^\top f(\vec{x}_2)}{\|f(\vec{x}_1)\| \|f(\vec{x}_2)\|} = \frac{\sum_{i=1}^d (f(\vec{x}_1)[i] \cdot f(\vec{x}_2)[i])}{\sqrt{\sum_{i=1}^d f(\vec{x}_1)[i]^2} \cdot \sqrt{\sum_{i=1}^d f(\vec{x}_2)[i]^2}} \quad (6)$$

and $f(\vec{x})[i]$ indicates the i -th component of the embedding vector of the function x . The cosine distance between two function embeddings is $[-1, 1]$. Where 1 means exactly the same, -1 means completely different.

5. Experiments and Evaluation

We make an extensive evaluation of GraphMoco on different tasks to examine the performance.

Task1, Cross Platform Tests On Dataset1: In this test, we evaluate how accurate is GraphMoco in BCSD tasks with different methods on a public available dataset.

Task2, Function search Tests On Dataset2: In the second task, we significantly increased the difficulty and we tested GraphMoco in a more common scenario. Given a certain binary function, we have to find the similes on a large dataset generated by several compilers.

Task 3 - Vulnerability Search on Dataset3: In this task, we evaluate our model on a real-world scenario. We search for vulnerable functions from the firmware that contain vulnerabilities .

Task 4 - Ablation Analysis: In this section, we quantify how different parts of

Algorithm 1 Framework of Graph Moco.

Input:

The set of positive samples for the current batch, $\{x_i\}_1^n$; the temperature constant τ ; a siamese network of the encoder for query and key $f_q(), f_k()$; the data augmentation function $Trans()$, momentum update parameter m ;

Output:

- 1: initialize the encoder for query and key, the parameters of both networks are identical $f_k() = f_q()$
 - 2: **for** each minibatch samples with n samples $\{x_i\}_1^n$ **do**
 - 3: Given one batch samples $\{x_i\}_1^N$, two augmented batches are generated $\{x_i^q\}_1^N, \{x_i^k\}_1^N$ with the augmentation function $Trans(\{x_i\}_1^n)$.
 - 4: Patch all the sub-graph $\{x_i^q\}_1^N$ into one large graph X_i^q . shuffle the sample order in the $\{x_i^k\}_1^N$ mini-batch, and patch all the sub-graph of $\{x_i^k\}_1^N$ into another large graph X_i^k .
 - 5: Encode the large graph pair with the siamese network, $\vec{X}^q = f_q(\vec{X}^q), \vec{X}^k = f_k(\vec{X}^k)$,
 - 6: Dispatch the \vec{X}^q to get the query embedding of each samples $f_q(\vec{x}_i^q)$, dispatch the \vec{X}^k and reshuffle sampler order to get the key embedding for each samples $f_k(\vec{x}_i^q)$
 - 7: Calculate the loss function $loss = \text{InfoNCE}(f_q(\vec{x}_i^q), f_k(\vec{x}_i^q))$, and update the parameters of the query encoder.
 - 8: Update the key encoder with $f_k.params = m * f_k.params + (1 - m) * f_q.params$
 - 9: **end for**
 - 10: **return** finetuned network f ;
-

GraphMoco contribute to the final results.

5.1. Setups

Setup. Our experimental environment is set up on a Linux server, running Ubuntu 20.04, equipped with two Intel Xeon 4210r CPUs at 2.4Ghz (each CPU has 10 cores and 20 virtual cores), 128G memory, and 1 Nvidia RTX 3090 GPU (24G memory). The software environment is Python 3.8 and PyTorch 1.11.0 with CUDA 11.7.

Hyperparameters. We implement our GraphMoco model with the follow setting. The total number of epochs that we will finetune the model is 100, the temperature is 0.07, and the dimension of the output embedding is 256. The learning rate is set to 0.01, and the adm optimizer is used. We train the model with a weight decay of $1e-4$ and we use a batch size of 128. The embedding dictionary size is 5120, and the momentum of dictionary is 0.999.

Metrics. In practice, we use function pairs that are compiled from the same source code as similar ones. This saves a lot of manual labelling effort, and it is also a common practice in academia [8] [24]. We use the cosine similarity function to measure the distance between the embedding vectors of two functions.

5.2. Task1: Cross Platform Tests On Dataset1

Dataset-1 consists of seven popular opensource projects: ClamAV, Curl, Nmap, OpenSSL, Unrar, Z3, and Zlib. Once compiled, they produce 24 different libraries. Each library is compiled using two compiler families, GCC and Clang, each with four different versions, covering major releases from 2015 to 2021 (more details on the opensource projects and compiler versions are provided in [20].) Each library is compiled for three different architectures, x86-64, ARM, and MIPS, in 32 and 64 bit versions (with a total of 6 architecture combinations), and 5 optimization levels O0, O1, O2, O3, and Os. To this end, we identify 7 different tasks to be evaluated: (1) arch: the function pairs have different architectures. (2) opt: the function pairs have different optimizations, but the same compiler, compiler version, and architecture. (3) comp: the function pairs have different compilers. (4) XC: the function pairs have different compilers, compiler versions, and optimizations, but the same architecture

and bitness. (5) XC+XB: the function pairs have different compiler, compiler versions, optimizations, and bitness, but the same architecture. (6) XA: the function pairs have different architectures and bitness, but the same compiler, compiler version, and optimizations. (7) XM: the function pairs are from arbitrary architectures, bitnesses, compilers, compiler versions, and optimization levels.

If the distance between the function pairs is less than a certain threshold, we will label the two functions as different. However, we do not use a specific threshold to assess the robustness of the detection model, but use other metrics, such as the AUC-ROC mechanism. For the most complex xm task, we use three metrics to evaluate the results: AUC, MRR10, RECALL@1. For other tasks we use only AUC.

Table 1: Results on function pairs across architectures, optimizations, and obfuscations.

model name	Description	XA	XC	XC+XB	XM	arch	comp	opt	XM	
									MRR10	Recall@1
GraphMoco	with StrandCNN	0.87	0.87	0.87	0.87	0.99	0.79	0.96	0.572	0.505
GGSNN	NoFeatures	0.82	0.82	0.83	0.82	0.93	0.79	0.84	0.37	0.29
GGSNN	OPC-2000	0.86	0.86	0.87	0.87	0.97	0.80	0.88	0.52	0.44
GMN	cfg+bow opc200	0.86	0.86	0.87	0.87	0.97	0.82	0.89	0.53	0.45
GMN	cfg	0.86	0.85	0.86	0.86	0.99	0.77	0.89	0.43	0.33
Gemini	GeminiFeatures	0.80	0.81	0.82	0.81	0.96	0.72	0.84	0.36	0.28
Gemini	NoFeatures	0.69	0.69	0.70	0.70	0.76	0.66	0.69	0.12	0.07
Gemini	OPC-200	0.78	0.81	0.82	0.81	0.93	0.74	0.85	0.369	0.26
GNN	ArithMean	0.74	0.79	0.79	0.77	0.88	0.73	0.83	0.25	0.16
GNN	AttentionMean	0.76	0.79	0.79	0.77	0.88	0.72	0.80	0.29	0.20
SAFE	ASM-list_250_e5	0.82	0.82	0.83	0.83	0.94	0.76	0.83	0.22	0.09
SAFE	ASM-list_Rand_Trainable_e10	0.79	0.79	0.80	0.80	0.94	0.70	0.81	0.28	0.17
SAFE	ASM-list_Trainable_e10	0.80	0.80	0.80	0.81	0.95	0.71	0.82	0.29	0.15
Trex	512tokens	0.73	0.80	0.79	0.77	0.87	0.80	0.89	0.31	0.25
asm2vec	e10	0.62	0.81	0.74	0.69	0.74	0.92	0.96	0.14	0.09

The results of our models are reported in Table 1. We can see that GraphMoco outperformed all the existing models almost in all the tests except the comp one. For the simplest different text **arch** GraphMoco achieved almost 100% accuracy. There is little difference between GraphMoco and the existing

SOTA model in terms of the AUC metrics. Our models significantly outperform the existing SOTA models GMN [18] on the MRR10 and recall@1 metrics, GraphMoco achieves 0.57 and 0.51, while the GMN model achieves 0.52 and 0.45. The results indicate that GraphMoco has more advantages in complex tasks.

5.3. Task2: Function Search Tests

In Task 1, we explore the capabilities of the model in a comprehensive way. The previous task used relatively small pool sizes of about 100. Considering that in real applications the pool size is often very large. Therefore, in Task 2 we focused on increasing the difficulty. Our main goal is to find ten functions that are semantically identical to the target function out of 10,000 functions. Compared to Task 1, the difficulty of Task2 has increased significantly.

The dataset is adapted from a big data competition run by 360 and National Engineering Research Center for Big Data Collaborative Security Technology ¹. There are 70,000 functions, each marked with a function id. The functions were compiled by three different compilers *gcc*, *llvm*, *clang*, three different CPU architectures, two bit types, and 5 different levels of optimisation. Over 2.4 million samples were compiled, with an average of over thirty samples per function. We split the dataset into train, validation and test dataset. There are 50,000 functions and about 1,600,000 samples in the training set, 3,000 functions with 100,000 samples in the validation set and 17,000 functions with 500,000 samples in the test set. We measure the performance using Mean Average Precision *MAP*. *AP* is the average accuracy of one prediction result, as shown in Equation 7.

$$AP = \frac{\sum_{k=1}^n (P(k) \times rel(k))}{N_{rel}} \quad (7)$$

where n is the total number of prediction functions, and n is set to 10 in this task; k is the ranking position of the prediction functions; $P(k)$ is the percentage of the first k prediction functions that are truly relevant; $rel(k)$ indicates whether

¹<https://www.datafountain.cn/competitions/593>

the k th prediction function is relevant, and relevant is 1, and vice versa is 0; N_{rel} indicates the total number of truly relevant functions in the test dataset. MAP is the mean value of the average accuracy of the multiple prediction results, where q is the serial number of the prediction, Q is the total number of predictions, and $AP(q)$ is the average accuracy of the q th prediction result.

$$MAP = \frac{\sum_{q=1}^Q AP(q)}{Q} \quad (8)$$

Table 2: Results of Task 2 On Test Dataset

model name	Description	MAP
GraphMoco	StrandCnn	0.91
Gemini	cfg	0.18
Gemini	embedding	0.23
GCN	CFG +bow opc 200	0.35
GAT2	CFG +bow opc 200	0.45
TREX	512tokens	0.76
Func2vec[27]	512tokens	0.86
SAFE	ASM-list_Trainable_e10	0.55
TikNIb[14]	Interpretable Feature	0.18

Due to the substantially increased difficulty of the test, the existing model did not do well on Test 2, with only the bert-based model [24][27] make a score above 0.6. GrapMoco still achieved a score of 0.91.

5.4. Task3: Vulnerability Search

Table 3: VULNERABILITIES WE HAVE CONFIRMED(✓) IN FIRMWARE IMAGES

CVE	Description	function name	TP-Link Deco-M4	NETGEAR R7000
CVE-2019-1563	Decrypt encrypted message	MDC2_Update	✓	✓
CVE-2019-1563	Decrypt encrypted message	PKCS7_dataDecode	✓	✓
CVE-2016-6303	Integer overflow	MDC2_Update	✓	
CVE-2016-2182	Allows denial-of-service	BN_bn2dec	✓	✓
CVE-2016-2176	Buffer over-read	X509_NAME_oneline		✓
CVE-2016-2106	Integer overflow	EVP_EncryptUpdate		✓
CVE-2016-2105	Integer overflow	EVP_EncodeUpdate		✓
CVE-2016-0798	Allows denial-of-service	SRP_VBASE_get_by_user		✓
CVE-2016-0797	NULL pointer dereference	BN_dec2bn		✓
CVE-2016-0797	NULL pointer dereference	BN_hex2bn		✓

In this task, we evaluate our model in a real-world scenario, finding functions that contain n-day vulnerabilities in firmware images. Firmware images often contain many third-party libraries, but when the libraries are patched, the firmware images are often updated very late or not updated at all. In this task, we use the dataset published by [20]. There are ten carefully selected vulnerable functions from OpenSSL1.0.2d, covering a total of eight CVEs. The targeted(key) functions are from the libcrypto libraries embedded in two firmware images: Netgear R7000 (ARM 32-bit) and TP-Link Deco M4 (MIPS 32-bit). There are 4 vulnerabilities for the Netgear R7000 and 9 for the TP-Link Deco M4. We list in detail the vulnerabilities that are contained in the firmware. We extracted 1,708 functions in the TP-Link Deco M4 and 1,776 functions in the Netgear. The extracted functions are compared to the above 10 functions which contain 7 vulnerabilities. We use the MRR10 as a comparison metric. The results show that our model significantly outperforms the existing SOTA model in most of cases (6 out of 8, about 9% on average), and only slightly underperforms the SOTA model in a few indicators (2 out of 8, about 2% on average).

Table 4: Results MRR10 of Vulnerability test.

model name	Description	Netgear R7000				TP-Link Deco-M4			
		x86	x64	ARM32	MIPS32	x86	x64	ARM32	MIPS32
GraphMoco	with TEXTCNN	0.88	0.63	1	0.88	0.65	0.92	0.67	0.85
GMN	cfg+bow ope200	0.88	0.54	1	0.79	0.67	0.73	0.70	0.78
GMN	cfg	0.65	0.43	0.69	0.54	0.80	0.88	0.88	0.98
GNN-s2v_GeminiNN	GeminiFeatures	0.33	0.042	0.38	0.25	0.11	0.26	0.28	0.11
GNN-s2v_GeminiNN	NoFeatures	0.0	0.0	0.028	0.0	0.0	0.0	0.11	0.0
GNN-s2v_GeminiNN	OPC-200	0.33	0.31	0.67	0.34	0.39	0.28	0.36	0.59
GNN-s2v	ArithMean_e5	0.1	0.08	0.5	0.0	0.05	0.06	0.028	0.18
GNN-s2v	AttentionMean_e5	0.05	0.03	0.04	0.0	0.0	0.03	0.04	0.27
SAFE	ASM-list_250_e5	0.0	0.0	0.0	0.0	0.04	0.02	0.07	0.03
SAFE	ASM-list_Rand_Trainable_e10	0.0	0.0	0.0	0.03	0.06	0.16	0.11	0.07
SAFE	ASM-list_Trainable_e10	0.08	0.29	0.29	0.16	0.04	0.16	0.24	0.09
Trex	512tokens	0.40	0.48	0.44	0.5	0.29	0.42	0.22	0.61
asm2vec	e10	0.25	0.13	0.86	0.5	0.11	0.11	0.02	0.67

5.5. Ablation

In this section we quantify how different parts of GraphMoco contribute to the final result. We evaluate 3 tasks. The first one is the preshuffle mechanism. The second one is the contrastive loss. The last one is with and without contrastive learning.

5.5.1. The effect of the StrandCNN encoder

To further investigate the impact of strandcnn, we compared the differences between strandcnn and other encoders. The results show that the use of strandcnn is more effective than. The good effect compared to fasttext is due to our presence. and zeek works well, probably because we make reasonable use of the features in terms of graph structure. The results show that zeek is only slightly weaker than graphmoco in the auc metric, and in the mrr10, recall1 metric, the zeek model lags substantially. This is because graphmoco uses a large number of graph features in addition to strand features. We also compared the results of using strandcnn with those of using ASM alone.

Table 5: Results on function pairs across architectures, optimizations, and obfuscations.

model name	Description	XA	XC	XC+XB	XM	arch	comp	opt	XM	
									MRR10	Recall@1
GraphMoco	with StrandCNN	0.87	0.87	0.87	0.87	0.99	0.79	0.89	0.572	0.505
Zeek	Strands	0.84	0.84	0.85	0.84	0.95	0.79	0.87	0.28	0.13

5.5.2. The Preshuffle Mechanism

To demonstrate the role of preshuffle mechanism, we trained the Task 2 by removing the preshuffle mechanism. Figure 6 provides the training and the test curves of GraphMoCo with or without preshuffle BN. As shown in the diagram, the dotted line indicates the effect without the preshuffle mechanism. The blue colour indicates performance in the test set. Removing preshuffle BN shows obvious overfitting to the pretext task: training accuracy of the pretext task quickly increases to 99%. But the test accuracy drops soon. The accuracy of training with the preshuffle mechanism improved slowly, but the results on the test set did not drop significantly. Without preshuffle mechanism, the model would learn cheating results. We can see that without the preshuffle mechanism, training accuracy of the model quickly increases to more than 99%. But the testing accuracy is very low about 14%. The results illustrated that without the preshuffle mechanism, the statistics in each batch would tell the model where the key embedding is. The preshuffle mechanism could stop the model from leaking information.

5.5.3. The Effect of the Contrastive Learning

We evaluate the performance of GraphMoco with the traditional supervise-learning model and triplet loss[29] model. In this test, we encode the function with the same encoder as GraphMoco. We just fine-tune the model with different methods. For supervise-learning model, we keep the ratio between similar and dissimilar function pairs in the finetuning set as roughly 1:5. It follows the setting of [24]. We test the model on Dataset2, and we follow the same setting

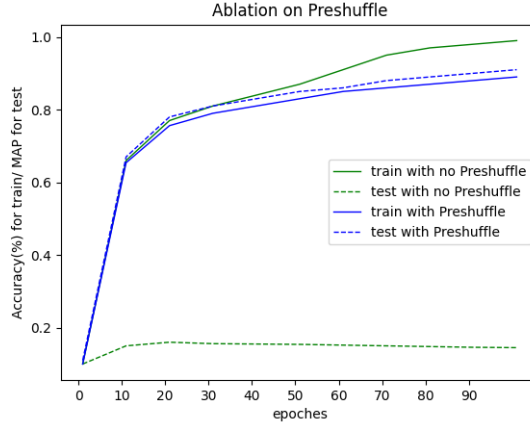


Figure 6: Figure provides the training and the test curves of GraphMoCo with or without preshuffle BN. As shown in the diagram, the blue colour indicates the effect with the preshuffle mechanism, the green colour indicates the effect without the preshuffle mechanism. The dotted line indicates performance in the test set.

as Task 2. The result shows that the accuracy of our model is 10 percentage points higher than the accuracy of traditional models.

6. Discussion & Conclusion

Our goal is to design a model that can be used in real-world scenarios while maintaining a high level of accuracy. A usable and applicable BCSD model often needs to run efficiently on massive amounts of data. So we design a simple CNN base encoder which is named StrandCNN. At the same time, we design a graph based momentum contrastive learning model that utilizes the preshuffle mechanism to solve the problem of shortcuts learned in pretext tasks. By using structural features at different levels, we achieve SOTA on multiple datasets with multiple metrics. Our model has advantages in terms of memory and computational complexity. We hope that our work can inspire others.

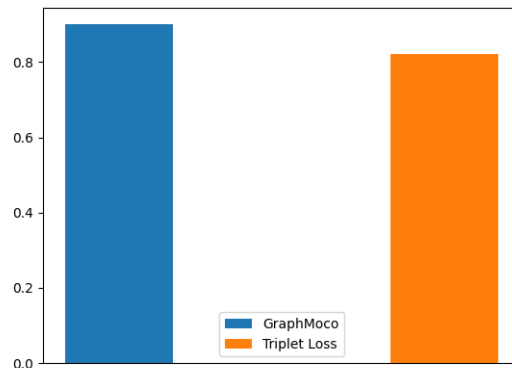


Figure 7: The framework of the proposed unsupervised learning method GraphMoco. It consists of a data augmentation part, a siamese network encoder and an embedding queue. The input function pairs are projected into a low-dimensional normalized embedding with the DNN based encoders. The query encoder is updated by back-propagation and the key encoder is updated by momentum.

References

- [1] Sunwoo Ahn, Seong Jin Ahn, Hyungjoon Koo, and Yunheung Paek. Practical binary code similarity detection with bert-based transferable similarity learning. *Proceedings of the 38th Annual Computer Security Applications Conference*, 2022.
- [2] Brenda S. Baker, Udi Manber, and Robert Muth. Compressing differences of executable code. In *In ACM SIGPLAN 1999 Workshop on Compiler Support for System Software (WCSS'99)*, 1999.
- [3] B.S. Baker. On finding duplication and near-duplication in large software systems. In *Proceedings of 2nd Working Conference on Reverse Engineering*, pages 86–95, 1995. doi: 10.1109/WCRE.1995.514697.
- [4] Mikhail Bilenko and Raymond J. Mooney. Adaptive duplicate detection using learnable string similarity measures. In *Proceedings of the Ninth ACM*

- SIGKDD International Conference on Knowledge Discovery and Data Mining*, KDD '03, page 39–48, New York, NY, USA, 2003. Association for Computing Machinery. ISBN 1581137370. doi: 10.1145/956750.956759. URL <https://doi.org/10.1145/956750.956759>.
- [5] Yaniv David, Nimrod Partush, and Eran Yahav. Statistical similarity of binaries. page 15.
- [6] Jacob Devlin, Ming-Wei Chang, Kenton Lee, and Kristina Toutanova. BERT: pre-training of deep bidirectional transformers for language understanding. *CoRR*, abs/1810.04805, 2018. URL <http://arxiv.org/abs/1810.04805>.
- [7] Jacob Devlin, Ming-Wei Chang, Kenton Lee, and Kristina Toutanova. BERT: Pre-training of deep bidirectional transformers for language understanding. In *Proceedings of the 2019 Conference of the North American Chapter of the Association for Computational Linguistics: Human Language Technologies, Volume 1 (Long and Short Papers)*, pages 4171–4186, Minneapolis, Minnesota, June 2019. Association for Computational Linguistics. doi: 10.18653/v1/N19-1423. URL <https://aclanthology.org/N19-1423>.
- [8] Steven H. H. Ding, Benjamin C. M. Fung, and Philippe Charland. Asm2vec: Boosting static representation robustness for binary clone search against code obfuscation and compiler optimization. In *2019 IEEE Symposium on Security and Privacy (SP)*, pages 472–489. IEEE. ISBN 978-1-5386-6660-9. doi: 10.1109/SP.2019.00003. URL <https://ieeexplore.ieee.org/document/8835340/>.
- [9] Sebastian Eschweiler, Khaled Yakdan, and Elmar Gerhards-Padilla. discover: Efficient cross-architecture identification of bugs in binary code. 02 2016. doi: 10.14722/ndss.2016.23185.
- [10] Kaiming He, Haoqi Fan, Yuxin Wu, Saining Xie, and Ross Girshick. Momentum contrast for unsupervised visual representation learning. page 10.

- [11] Geoffrey Hinton, Oriol Vinyals, and Jeff Dean. Distilling the knowledge in a neural network, 2015.
- [12] Sergey Ioffe and Christian Szegedy. Batch normalization: Accelerating deep network training by reducing internal covariate shift. In *Proceedings of the 32nd International Conference on International Conference on Machine Learning - Volume 37*, ICML'15, page 448–456. JMLR.org, 2015.
- [13] Wei Ming Khoo, Alan Mycroft, and Ross Anderson. Rendezvous: A search engine for binary code. In *2013 10th Working Conference on Mining Software Repositories (MSR)*, pages 329–338. IEEE. ISBN 978-1-4673-2936-1 978-1-4799-0345-0. doi: 10.1109/MSR.2013.6624046. URL <http://ieeexplore.ieee.org/document/6624046/>.
- [14] Dongkwan Kim, Eunsoo Kim, Sang Kil Cha, Sooel Son, and Yongdae Kim. Revisiting binary code similarity analysis using interpretable feature engineering and lessons learned. *IEEE Transactions on Software Engineering*, 49(4):1661–1682, apr 2023. doi: 10.1109/tse.2022.3187689. URL <https://doi.org/10.1109%2Ftse.2022.3187689>.
- [15] Yoon Kim. Convolutional neural networks for sentence classification. *Proceedings of the 2014 Conference on Empirical Methods in Natural Language Processing*, 08 2014. doi: 10.3115/v1/D14-1181.
- [16] Hyungjoon Koo, Soyeon Park, Daejin Choi, and Taesoo Kim. Semantic-aware binary code representation with BERT. *CoRR*, abs/2106.05478, 2021. URL <https://arxiv.org/abs/2106.05478>.
- [17] Xuezixiang Li, Qu Yu, and Heng Yin. PalmTree: Learning an assembly language model for instruction embedding. URL <http://arxiv.org/abs/2103.03809>.
- [18] Yujia Li, Chenjie Gu, Thomas Dullien, Oriol Vinyals, and Pushmeet Kohli. Graph matching networks for learning the similarity of graph structured objects. *ArXiv*, abs/1904.12787, 2019.

- [19] Chao Liu, Chen Chen, Jiawei Han, and Philip S. Yu. Gplag: Detection of software plagiarism by program dependence graph analysis. In *In the Proceedings of the 12th ACM SIGKDD International Conference on Knowledge Discovery and Data Mining (KDD'06)*, pages 872–881. ACM Press, 2006.
- [20] Andrea Marcelli, Mariano Graziano, Xabier Ugarte-Pedrero, Yanick Fratantonio, Mohamad Mansouri, and Davide Balzarotti. How machine learning is solving the binary function similarity problem. In *31st USENIX Security Symposium (USENIX Security 22)*, pages 2099–2116, Boston, MA, August 2022. USENIX Association. ISBN 978-1-939133-31-1. URL <https://www.usenix.org/conference/usenixsecurity22/presentation/marcelli>.
- [21] Luca Massarelli, Giuseppe Antonio Di Luna, Fabio Petroni, Leonardo Querzoni, and Roberto Baldoni. SAFE: Self-attentive function embeddings for binary similarity. URL <http://arxiv.org/abs/1811.05296>. Number: arXiv:1811.05296.
- [22] Tomas Mikolov, Ilya Sutskever, Kai Chen, Greg Corrado, and Jeffrey Dean. Distributed representations of words and phrases and their compositionality. In *Proceedings of the 26th International Conference on Neural Information Processing Systems - Volume 2, NIPS'13*, page 3111–3119, Red Hook, NY, USA, 2013. Curran Associates Inc.
- [23] Christopher Morris, Martin Ritzert, Matthias Fey, William L. Hamilton, Jan Eric Lenssen, Gaurav Rattan, and Martin Grohe. Weisfeiler and leman go neural: Higher-order graph neural networks. In *Proceedings of the Thirty-Third AAAI Conference on Artificial Intelligence and Thirty-First Innovative Applications of Artificial Intelligence Conference and Ninth AAAI Symposium on Educational Advances in Artificial Intelligence, AAAI'19/IAAI'19/EAAI'19*. AAAI Press, 2019. ISBN 978-1-57735-809-1. doi: 10.1609/aaai.v33i01.33014602. URL <https://doi.org/10.1609/aaai.v33i01.33014602>.

- [24] Kexin Pei, Junfeng Yang, Zhou Xuan, and Suman Jana. TREX: Learning execution semantics from micro-traces for binary similarity. page 19.
- [25] Jannik Pewny, Felix Schuster, Lukas Bernhard, Thorsten Holz, and Christian Rossow. Leveraging semantic signatures for bug search in binary programs. In *Proceedings of the 30th Annual Computer Security Applications Conference, ACSAC '14*, page 406–415, New York, NY, USA, 2014. Association for Computing Machinery. ISBN 9781450330053. doi: 10.1145/2664243.2664269. URL <https://doi.org/10.1145/2664243.2664269>.
- [26] Jannik Pewny, Behrad Garmany, Robert Gawlik, Christian Rossow, and Thorsten Holz. Cross-architecture bug search in binary executables. In *2015 IEEE Symposium on Security and Privacy*, pages 709–724, 2015. doi: 10.1109/SP.2015.49.
- [27] Sun RuiJin, Guo ShiZe, Guo JinHong, Sun Meng, and Pan ZhiSong. Fun2vec:a contrastive learning framework of function-level representation for binary, 2022.
- [28] Alberto Sanfeliu and King-Sun Fu. A distance measure between attributed relational graphs for pattern recognition. *IEEE Transactions on Systems, Man, and Cybernetics*, SMC-13(3):353–362, 1983. doi: 10.1109/TSMC.1983.6313167.
- [29] Florian Schroff, Dmitry Kalenichenko, and James Philbin. FaceNet: A unified embedding for face recognition and clustering. In *2015 IEEE Conference on Computer Vision and Pattern Recognition (CVPR)*. IEEE, jun 2015. doi: 10.1109/cvpr.2015.7298682. URL <https://doi.org/10.1109/2Fcvpr.2015.7298682>.
- [30] Noam Shalev and Nimrod Partush. Binary similarity detection using machine learning. In *Proceedings of the 13th Workshop on Programming Languages and Analysis for Security, PLAS '18*, page 42–47, New York, NY, USA, 2018. Association for Computing Machinery. ISBN

9781450359931. doi: 10.1145/3264820.3264821. URL <https://doi.org/10.1145/3264820.3264821>.

- [31] Aäron van den Oord, Yazhe Li, and Oriol Vinyals. Representation learning with contrastive predictive coding. *CoRR*, abs/1807.03748, 2018. URL <http://arxiv.org/abs/1807.03748>.
- [32] Ashish Vaswani, Noam Shazeer, Niki Parmar, Jakob Uszkoreit, Llion Jones, Aidan N. Gomez, Lukasz Kaiser, and Illia Polosukhin. Attention is all you need. In *Proceedings of the 31st International Conference on Neural Information Processing Systems, NIPS'17*, page 6000–6010, Red Hook, NY, USA, 2017. Curran Associates Inc. ISBN 9781510860964.
- [33] Hao Wang, Wenjie Qu, Gilad Katz, Wenyu Zhu, Zeyu Gao, Han Qiu, Jianwei Zhuge, and Chao Zhang. jtrans: Jump-aware transformer for binary code similarity, 2022.
- [34] Zhirong Wu, Yuanjun Xiong, Stella X. Yu, and Dahua Lin. Unsupervised feature learning via non-parametric instance discrimination. In *2018 IEEE/CVF Conference on Computer Vision and Pattern Recognition*, pages 3733–3742. IEEE. ISBN 978-1-5386-6420-9. doi: 10.1109/CVPR.2018.00393. URL <https://ieeexplore.ieee.org/document/8578491/>.
- [35] Keyulu Xu, Weihua Hu, Jure Leskovec, and Stefanie Jegelka. How powerful are graph neural networks? *CoRR*, abs/1810.00826, 2018. URL <http://arxiv.org/abs/1810.00826>.
- [36] Xiaojun Xu, Chang Liu, Qian Feng, Heng Yin, Le Song, and Dawn Song. Neural network-based graph embedding for cross-platform binary code similarity detection. page 14.
- [37] Fabian Yamaguchi, Nico Golde, Daniel Arp, and Konrad Rieck. Modeling and discovering vulnerabilities with code property graphs. In *2014 IEEE Symposium on Security and Privacy*, pages 590–604, 2014. doi: 10.1109/SP.2014.44.

- [38] Zeping Yu, Rui Cao, Qiyi Tang, Sen Nie, Junzhou Huang, and Shi Wu. Order matters: Semantic-aware neural networks for binary code similarity detection. 34(1):1145–1152. ISSN 2374-3468, 2159-5399. doi: 10.1609/aaai.v34i01.5466. URL <https://aaai.org/ojs/index.php/AAAI/article/view/5466>.